A new mathematical model for traveling sand dunes: analysis and approximation

M. Falcone S. Finzi Vita

Abstract. We present a new two-layer closed form model for the dynamics of desert dunes under the effect of a horizontal wind blowing in an arbitrary direction. This model is an extension of a very simplified model previously introduced by Hadeler and Kuttler [12]. Our extension, inspired by the sandpile dynamics approach, includes the effects of gravity on both sides (upwind and downwind) of the dune, and allows to describe erosion and deposition in more accurate way. After a discussion of the model and its properties we present a numerical scheme based on finite differences in the simplified 2D settings and we prove its consistency and stability. Some numerical tests show a good qualitative behavior and a realistic shape for the evolving dunes. Finally, we discuss the preliminary steps of a possible extension of this model to the 3D case.

1 Introduction

The evolution of dunes is a rather complex phenomenon involving several features of granular materials. In particular, it is crucial to describe in the model the erosion and deposition of sand grains since this is the driving force for the dune evolution under the wind action. Clearly these effects are different on the two sides of the dune and one has to distinguish between the up-wind side and the down-wind side. In the up-wind side (*the luff*) erosion is dominant whereas in the down-wind side (*the lee*) the deposition is more important and some avalanches can appear. Other important elements and forces contributing to the modeling of the dune shape are the gravity force, the sand availability and the critical slope associated to the sand (the latter varies depending on the diameter and characteristic of the grains/pebbles forming the dunes). Many of these physical features have been described in the pioneering work of Bagnold [3] who gave a rather complete description of the variety of shapes appearing in the dune evolution and examined the dependence of the shape evolution on the above features. A detailed analysis of the phenomenon can be also found for example in [1].

In this paper we propose an extension of the so-called two layers model (also named BCRE model after the names of its authors [4]) to the dune evolution; in this effort we will also take advantage of the our previous works on the construction of the sand piles via the two layers approach for the open table problem [6].

The BCRE system of PDEs is the mathematical translation of a simple model that has been proposed in [4] for the description of avalanche flows on the surface of a granular medium. The flow is modeled as a *rolling layer* moving on a fixed bed of solid particles, called *standing layer*. The dynamics is described by two coupled phenomenological equations. Denoting by w the height of the moving (rolling) layer and h the height of the standing layer, the dynamics can be characterized by two main phenomena:

- the *transport* of the rolling layer, i.e. the movement of the sand driven by an advection force with mean velocity V;
- the *deposition*, i.e. the conversion of the moving grains into a static state which is described by a quantity $\Gamma(w,h)$ representing the exchange between the rolling and the standing layer. Actually, this quantity plays a role of an absorption for the transport of the rolling layer and a reaction for the standing one.

More precisely, the dynamics can be described by the following system of evolutive partial differential equations

$$\begin{cases} \partial_t w = \nabla \cdot (w\, V) - \Gamma(w,h) + f \\ \\ \partial_t u = \Gamma(w,h) \end{cases} \tag{1}$$

where f represents an external source of the sand (or granular matter). The quantities V and $\Gamma(w,h)$ need to be defined with respect to the assumptions on the problem.
Model (1) has been improved by Hadeler and Kuttler [11] in order to describe sandpile formation under gravity source on a bounded open table, or over a silo of bounded cross-section. In their model the grains in the rolling layer move downhill at a velocity proportional to the slope of the standing layer, that is $V = -\beta\nabla h$, and the exchange term takes the form

$$\Gamma(w,h) = \gamma(\alpha - |\nabla h|)w,$$

where α denotes the tangent of the angle of repose of the granular material (tipically $\alpha \simeq 34°$ for dry sand) and γ is a constant exchange rate. When the slope of the heaps exceeds α avalanches begin and previously stationary grains leaves the standing layer entering the rolling one. On the contrary, rolling grains stop and deposit when they reach a region where the standing layer is less steep than α. It is worth to say that different models for the description of sandpile dynamics have been proposed for example in [18], and more recently in [16].
In order to extend the two layer approach to the dynamics of a desert dune one has to add to the model the effects of the blowing wind. The simple situation we have in mind is the formation and the evolution of the so-called barchan dunes, which appears when the wind always blowing in the same horizontal direction on a surface with low availability of sand.
Rather efficient models for dune dynamics have been extensively studied in the literature (see for example [19], [15], [13], [17], [2], [9]). Taking advantage of the different time scales of the involved phenomena, in this kind of models the global dynamics is obtained by successive steps: the computation of the shear stress for a given dune profile, the determination of the sand flux corresponding to the shear stress, the solution of the mass conservation equation for the given sand flux and finally the correction due to possible avalanches effects. To follow the evolution of a dune, this sequence has to be repeated for any time step of discretization. As an example of that we recall in Section 2.1 the Minimal Model of Kroy, Sauermann and Herrmann [15], which is a simplified version of the continuum saltation model described in [19].
Looking for a single system of equations able to describe the global evolution of the dune (at least at a qualitative level), Hadeler and Kuttler proposed in [12] a simplified 2D model taking into account the effects of erosion and deposition on the two distinguished layers of the dune, the standing and the moving ones (in analogy with the sandpile description).

In Section 2.2 we recall that basic model, for which the existence of a traveling solution in $\mathbb{R}$ can be proved. Numerical tests show the emergence of a finite time attractor profile even when this model is applied to the case of compact supported dunes.
Our goal is to modify the simple model of [12] in order to incorporate a more realistic sandpile dynamics derived from [11]. In this approach a single pair of partial differential equations of evolutive type for the two layers is able to take care of the whole phenomena: erosion, advection, deposition and avalanche effects. We describe this 2D new model in Section 3, its discretization based on finite differences and some properties of the schemes are presented in Section 4 and many numerical tests are illustrated in Section 5.
Finally in Section 6 we show a first attempt to extend such an approach to the complete 3D phenomenon of real dune evolution (of barchan type). We acknowledge the contribution of F. Haack for some of the numerical tests presented in this paper and for some helpful discussions we had during the development of her master thesis [10].

2 Two models from the literature

Due to the complicated nature of sand flux dynamics and dune migration, a number of mathematical models have been proposed with the aim of describing dune migration at a macroscopic level. Let us briefly describe two models for the dune evolution to compare our model with those existing in the literature.

2.1 The Minimal Model (Kroy, Sauermann and Herrmann [15])

In this section we recall the essential features of the so-called *Minimal Model for Sand Dunes* proposed by Kroy et al. in [15], a widely accepted simplified version of the complete continuum saltation model introduced in [19]. Since the dune's migration takes place on a much longer time scale than the sand transport dynamics, in this model the dune profile h is considered stationary for the calculation of the shear stress and the sand flux, giving rise to the following algorithm to be applied to every discrete time $\bar{t}$ (the quantities $\rho_{air}, \rho_{sand}, \rho_{dune}$ denote respectively the air, sand and dune densities):

1. *Calculate the shear stress $\tau(x,\bar{t}) = \tau(x)$ and consequently the shear velocity $u_*(x)$ at a given time $\bar{t}$ for a given profile $h(x,\bar{t})$.*

   The dune profile induces a perturbation of the shear stress with respect to that of a horizontal surface τ_0. Using the analytic theory of boundary perturbation (see e.g. [14] and [15]), the shear stress and velocity can be computed via the following formulas:

   $$\frac{\tau(x)}{\tau_0} = 1 + A\int_{\mathbb{R}} \frac{1}{\pi y} h_x(x-y)dy + Bh_x(x), \quad u_*(x) = \sqrt{\frac{\tau(x)}{\rho_{air}}}, \tag{2}$$

   with A and B suitable constants. If the dune also presents a slip face, that is to say, if the downwind slope of the dune exceeds 14°, then the shear stress is not calculated on h but rather on $\widetilde{h} = \max\{h, s\}$, where the *separating streamline* s is a function which indicates the boundary of the *separation bubble* in which the shear stress can be considered null (see Fig. 1). For the model, s is taken as a third-degree polynomial whose maximum slope does not exceed $\tan(14°)$.

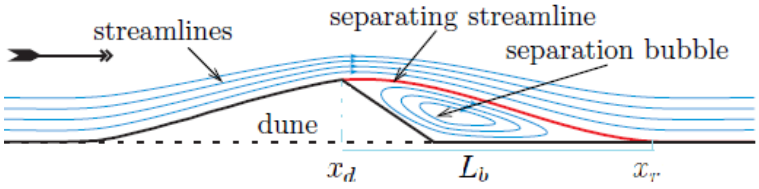

Figure 1: Separation bubble (from [15])

2. *Calculate the sand flux $q(x)$ for a given shear velocity $u_*(x)$.*

   The sand flux $q(x)$ is calculated using the relation

$$\frac{\partial q}{\partial x} = \frac{q_{sat} - q}{L_{sat}} \tag{3}$$

   where q_{sat} is the saturation flux given by Bagnold's formula (see [3])

$$q_{sat} = \frac{4}{3}\frac{C}{g}\rho_{air}u_*^3, \tag{4}$$

   and the saturation length $L_{sat} \approx 2d\frac{\rho_{sand}}{\rho_{air}}$. Note that erosion is possible only where the dune profile $h(x)$ is positive. Where this is not the case, we have simply $\frac{\partial q}{\partial x} = 0$.

3. *Calculate the new dune profile by solving the mass conservation equation at time $\bar{t}$ for the computed flux $q(x) = q(x, \bar{t})$, taking into account possible avalanche effects.*

   The true equation for the dune profile then becomes

$$\rho_{dune}\frac{\partial h}{\partial t}(x,t) = -\frac{\partial q}{\partial x}(x,t) \quad \text{subject to} \quad |h_x| \leq \alpha, \tag{5}$$

   where $\rho_{dune} = (1-\lambda)\rho_{sand}$ and $\lambda \in [0,1]$ is the porosity coefficient. The constraint $|h_x| \leq \alpha = \tan\theta$ has to be imposed since avalanches can occur when the dune profile exceed the maximum slope. In accordance with Caboussat and Glowinski [5], equation (5) can take the form of a variational inequality.

Summing up, the Minimal Model (which for simplicity we will refer to as Model M) consists in the successive resolution of equations (2)-(5) at each time step.

2.2 A 2D dune evolution model (Hadeler and Kuttler [12])

In 2003 Hadeler and Kuttler [12] presented an extremely simple, original model for two-dimensional migrating dunes based on the two-layer approach. As for the sandpile model described in [11], the dune is modeled as a thick, underlying standing layer $h(x,t)$ with a thin rolling layer $w(x,t)$ of moving grains above it. They assume that the wind blows from the left along the x axis at a constant speed, and that the dune has a single crest at the point $\widehat{x}(t)$ corresponding to its maximal heigth (moving with a constant speed c much lower than the wind speed). Clearly, the crest's speed will depend upon the wind speed, the dune size and the sand availability.

On the upwind side, the sand is taken up from the standing layer by the wind according to a constant erosion rate σ. On the downwind side, where the wind cannot entrain new grains, the sand is deposited from the moving layer into the standing layer with a constant deposition rate δ. In addition, the rolling layer is transported to the right with transport speed η, which of course depends on the wind speed. In their assumptions the speed is assumed to be the same on both sides of the crest. Although this seems to be unphysical, it simplifies the model.

In these simplified settings, the upwind and downwind sides of the dune are determined by the position of the crest $\widehat{x}$ or, which is equivalent, by the sign of the standing layer derivative, i.e. the upwind side (*the luff*) is where h_x is positive and the downwind side (*the lee*) is where h_x is negative.

Model A

$$\begin{cases} h_t = \begin{cases} -\sigma h & \text{if} \quad h_x > 0 \\ \delta w & \text{if} \quad h_x < 0 \end{cases} \\ w_t + \eta w_x = \begin{cases} \sigma h & \text{if} \quad h_x > 0 \\ -\delta w & \text{if} \quad h_x < 0 \end{cases} \end{cases} \tag{6}$$

with of course given initial data h_0 and w_0. Let us note that the entire dune, $h + w$, is simply transported, that is to say, the grains can move between the two layers, but the total volume of the dune is conserved. Indeed, for a smooth dune with compact support in a large interval $[a, b] \subset \mathbb{R}$ we have

$$\frac{d}{dt}\int_a^b (h+w)dx = \int_a^b (h_t + w_t)dx = \int_a^b -\eta w_x dx$$
$$= \int_a^{\widehat{x}} -\eta w_x dx + \int_{\widehat{x}}^b -\eta w_x dx = -\eta[w(b,t) - w(a,t)] = 0, \tag{7}$$

for the continuity of the rolling layer at the crest $\widehat{x}$ (here we assumed that the support of the dune stays in $[a, b]$ for every time $t < T$). Perhaps the most interesting aspect about sand dunes is that, under constant speed and constant direction of the wind, the shape of dune appearing during the evolution is always the same. For example, in case of a constant, unidirectional wind parallel to the x axis with no sand bed, we expect barchan dunes. Moreover, if the general wind conditions don't change so much, a consolidated dune tends to keep its shape in time. If a model is well written, this geological experience should have a mathematical counterpart in the presence of a *similarity solution*, that is to say, a particular dune profile that is rigidly transported with some constant speed c. The simplified model of HK exhibits this kind of solutions. If we allow for a single discontinuity in the slope of the dune at the crest, which we will assume to be located in $x = 0$ at time $t = 0$, then we look for a traveling dune of the form $h(x,t) + w(x,t) = H(\xi) + W(\xi)$, with $\xi = x - ct$. Since the crest also travels with speed c, the position of the crest (and of the resulting slope discontinuity) will be in $x = ct$ at time t. Thus, $\xi = 0$ is the crest, $\xi < 0$ and $\xi > 0$ denote respectively the upwind and the downwind side of the dune. Imposing that such a similarity solution satisfies equations (6), its explicit form can be derived (see [12] for details):

$$H(\xi) = \begin{cases} h_0 e^{\lambda \xi} & \xi < 0 \\ h_0 e^{-\mu \xi} & \xi > 0 \end{cases}, \qquad W(\xi) = \epsilon H(\xi) \tag{8}$$

where

$$\lambda = \frac{\sigma(1+\epsilon)}{\epsilon\eta}, \quad \mu = \frac{\delta(1+\epsilon)}{\eta}, \quad c = \frac{\epsilon\eta}{1+\epsilon}, \tag{9}$$

and $\epsilon = w_0/h_0$ denotes the relative height of the rolling layer with respect to the standing layer at the initial crest position (an example of such $H(\xi)$ for a specific choice of parameters is shown in Fig. 2).

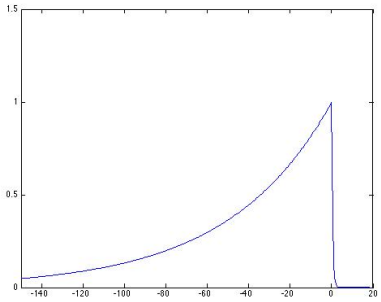

Figure 2: Traveling dune for Model A ($\epsilon = 10^{-2}$, $\sigma = 10^{-4}$, $\delta = 1$, $\eta = 0.5$, $h_0 = 1$)

Note that even if the shape strongly depends on the parameters, the final solution is always the composition of two exponential functions, one with a positive exponent before the crest, and one with a negative exponent after it. This means that the surface remains convex before and after the crest. Real barchan dunes have a steep convex lee side after the crest, but the upwind part of the dune switches from convex to concave approaching the crest. This seems to indicate that Model A is too simple to accurately describe real dunes. It is also interesting to note that for this model one observes that the evolution reaches a stable shape in finite time, which is only advected in the sequel.

3 A New 2D Dune Model

Model M is able to reproduce the dynamics of sand dunes, but it requires the solution of different successive equations. On the other side, due to its extreme simplicity, Model A loses many key elements of realistic dune migration.This has motivated our research for an extension of Hadeler and Kuttler's model with the aim to recover the simplicity of Model A while obtaining more realistic evolutions for the dunes.

As in the previous model, the dune is described as a standing layer and a rolling layer. The difference is that in this new model the creation and migration of a dune is due to two different phenomena: gravity, which makes grains in the rolling layer move downhill, and wind, which transports the eroded grains. Thus the objective is to write a BCRE model like (1) (with $f = 0$) and to determine Γ and V accordingly. More precisely their components due to the gravity force and to the wind contribute as follows:

$$\Gamma = \Gamma_g + \Gamma_w, \qquad V = V_g + V_w \ . \tag{10}$$

Let us look at each contribution separately. Without wind, the model is simply the Hadeler and Kuttler's 2D sandpile model studied in [11] with no source term, so that

$$\Gamma_g = \gamma(\alpha - |h_x|)w, \qquad V_g = -\beta h_x \ . \tag{11}$$

Let us observe that, in order to simplify the model, we identify the crest and the brink of the dune, although for small dunes usually the brink, i.e. the point where the deposition starts, is in the down-wind side separated from the crest [1]. Note that h_x is usually discontinuous at the brink.
Neglecting gravity, we can distinguish different phenomena on the luff side and on the lee side of the crest. On the first one the rolling layer is moved to the right by the wind according to a constant transport speed $\bar{\eta}$ and the sand is eroded from the standing layer and enters the rolling layer with an erosion rate σ (assumed constant).

On the lee side, on the other hand, the sand is deposited into the standing layer with a constant deposition rate δ. As for sand transport due to the wind, it is clear that moving grains on the lee side are at least partially blocked from the wind by the dune profile itself. For this reason, unlike Model A, we do not take a constant transport speed but rather one which linearly decreases to zero after the crest. Note that the dune partially blocks the wind for a distance proportional to the height of the dune. We take into account the protection given by the dune via the definition of the transport velocity $\eta(x)$ that will depend on point (before it was assumed to be constant).
The we define $\eta(x)$ as follows:

$$\eta(x) = \begin{cases} \bar{\eta} & x < \widehat{x} \\ \bar{\eta} - \frac{\bar{\eta}}{\mu h(\widehat{x})}(x - \widehat{x}) & \widehat{x} \le x \le \widehat{x} + \mu h(\widehat{x}) \\ 0 & x > \widehat{x} + \mu h(\widehat{x}) \end{cases} \tag{12}$$

The parameter μ controls the protection effect and says that the velocity vanishes at a certain distance from the crest, physical experiments show that the protection given by a crest of height $h(\widehat{x})$ covers a lenght of about $6h(\widehat{x})$ [15]. Since we are dealing with a single dune we simply ignore the transport on the lee far away from the crest. We will come back to this point in Section 5 dealing with multiple dunes.
In conclusion, the exchange term and the velocity due to the wind are:

$$h_x > 0: \begin{cases} \Gamma_w = -\sigma h \\ V_w = \eta(x) = \bar{\eta} \end{cases} \qquad h_x < 0: \begin{cases} \Gamma_w = \delta w \\ V_w = \eta(x) \end{cases} \tag{13}$$

Putting everything together, we obtain a new model, which we will refer to as Model B:

Model B

$$\begin{cases} h_t = \begin{cases} -\sigma h + \gamma(\alpha - |h_x|)w & \text{if } h_x > 0 \\ (\gamma(\alpha - |h_x|) + \delta)w & \text{if } h_x < 0 \end{cases} \\ \\ w_t = \begin{cases} (w(\beta h_x - \eta(x)))_x + \sigma h - \gamma(\alpha - |h_x|)w & \text{if } h_x > 0 \\ (w(\beta h_x - \eta(x)))_x - (\gamma(\alpha - |h_x|) + \delta)w & \text{if } h_x < 0 \end{cases} \end{cases} \tag{14}$$

Like Model A, Model B also conserves the volume of the dune. In fact, for a smooth dune $h + w$, taking into account (14), we have

$$\frac{d}{dt}\int_a^b (h + w)dx = \int_a^b (h_t + w_t)dx = \int_a^b (w(\beta h_x - \eta(x)))_x dx \tag{15}$$

and again, splitting the integral in two terms with respect to the crest position $\widehat{x}$, we get

$$\int_a^b (w(\beta h_x - \eta(x)))_x dx = \int_a^{\widehat{x}} (w(\beta h_x - \eta(x)))_x dx + \int_{\widehat{x}}^b (w(\beta h_x - \eta(x)))_x dx \tag{16}$$

$$= w(\widehat{x})(\beta h_x^-(\widehat{x}) - \eta^-(\widehat{x})) - w(\widehat{x})(\beta h_x^-(\widehat{x}) - \eta^+(\widehat{x})) = 0 \tag{17}$$

where f_x^- and f_x^+ represent respectively the left and right derivative of a function f. Note that in that calculation we have used the continuity of η and the fact that the sand is advected from the left, so at the crest we should consider the up-wind derivative of h. This implies that

$$\frac{d}{dt}\int_a^b (h + w)dx = 0 \tag{18}$$

also for Model B.

4 Finite difference schemes for Models A and B

Models A and B were discretized in the same way, using an upwind discretization for w_x and h_x and forward discrete time derivatives. We will consider an initial dune h_0 with compact support in some subset $[a, b] \subset \mathbb{R}$. At time $t = 0$, the wind begins to blow towards the right along the x axis with a constant speed. The initial rolling layer w_0 is then supposed to be zero at $t = 0$. We divide $[a, b]$ into N_x intervals of uniform width $\Delta x = \frac{b-a}{N_x}$. We then choose a final observation time T and divide the time interval $[0, T]$ into N_t intervals of uniform width $\Delta t = \frac{T}{N_t}$. With this notations, the spatial nodes becomes $x_j = a + j\Delta x$ for $j = 0, ..., N_x$ and the discrete times $t^n = n\Delta t$ for $n = 0, ..., N_t$. We will denote the approximate solutions h and w in node x_j at time t^n with h_j^n and w_j^n, respectively.

The schemes corresponding to the models are shown below.

FD scheme for Model A: For $j = 0, ..., N_x$, $n = 0, ..., N_t - 1$

$$\begin{cases} h_j^{n+1} = h_j^n + \Delta t S_j^n \\ w_j^{n+1} = w_j^n - \eta\frac{\Delta t}{\Delta x}\Big(w_j^n - w_{j-1}^n\Big) - \Delta t S_j^n \end{cases} \tag{19}$$

where

$$S_j^n = \begin{cases} -\sigma h_j^n & h_j^n \geq h_{j-1}^n \\ \delta w_j^n & h_j^n < h_{j-1}^n \end{cases} \tag{20}$$

represents the erosion or the deposition term, depending on whether the node x_j is upwind or downwind at time t^n.

FD scheme for Model B: For $j = 0, ..., N_x$, $n = 0, ..., N_t - 1$

$$\begin{cases} h_j^{n+1} = h_j^n + \Delta t S_j^n + \gamma\Delta t(\alpha - \left|\frac{h_j^n - h_{j-1}^n}{\Delta x}\right|)w_j^n \\ w_j^{n+1} = w_j^n - \frac{\Delta t}{\Delta x}\Big(w_j^n\phi_j^n - w_{j-1}^n\phi_{j-1}^n\Big) - \Delta t S_j^n - \gamma\Delta t(\alpha - \left|\frac{h_j^n - h_{j-1}^n}{\Delta x}\right|)w_j^n \end{cases} \tag{21}$$

where

$$\phi_j^n = \eta_j^n - \beta\frac{(h_j^n - h_{j-1}^n)}{\Delta x} \tag{22}$$

is the overall velocity of the rolling layer, and the transport speed η_j^n is defined on the grid according to (12).

As already said, the continuous schemes (6) and (14) both conserve the volume of the dune, since no grains are added or removed during the dune's migration. This fact is also true numerically, as the following theorem proves.

Theorem 4.1. *The schemes (19) and (21) are conservative, that is to say, $M(t^n) = M(t^0)$ for $n = 1, ..., N_t$, where*

$$M(t^n) := \Delta x \sum_{j=1}^{N_x} (h_j^n + w_j^n) \tag{23}$$

Proof. For Model A, we have that

$$\begin{aligned} M(t^{n+1}) =& \Delta x \sum_{j=1}^{N_x} \Big(h_j^n + w_j^n - \eta \frac{\Delta t}{\Delta x} (w_j^n - w_{j-1}^n) \Big) \\ =& M(t^n) - \eta \Delta t \sum_{j=1}^{N_x} (w_j^n - w_{j-1}^n) = M(t^n) - \eta \Delta t (w_{N_x}^n - w_0^n) = M(t^n), \end{aligned}$$

where in the last equality we have used the fact that w has compact support in $[a, b]$. By induction the theorem holds in this case. The same type of reasoning can be applied to Model B:

$$\begin{aligned} M(t^{n+1}) =& \Delta x \sum_{j=1}^{N_x} \Big(h_j^n + w_j^n - \frac{\Delta t}{\Delta x} (w_j^n \phi_j^n - w_{j-1}^n \phi_{j-1}^n) \Big) \\ =& M(t^n) - \Delta t \sum_{j=1}^{N_x} (w_j^n \phi_j^n - w_{j-1}^n \phi_{j-1}^n) = M(t^n) - \Delta t (w_{N_x}^n \phi_{N_x}^n - w_0^n \phi_0^n) = M(t^n). \end{aligned}$$

□

Concerning stability, the following results hold.

Theorem 4.2. *The scheme (19) for Model A (6) has the following properties:*
i) is consistent of order 1 in Δt and Δx;
ii) is stable for

$$\Delta t \leq \frac{2\Delta x}{2\eta + \delta \Delta x}. \tag{24}$$

.

Proof. i) Consistency
Let us examine the scheme first on the upwind side where $S_j^n \equiv -\sigma h_j^n$. This implies

$$\begin{cases} h_j^{n+1} = h_j^n - \Delta t \sigma h_j^n \\ w_j^{n+1} = w_j^n - \eta \frac{\Delta t}{\Delta x} \Big(w_j^n - w_{j-1}^n \Big) + \Delta t \sigma h_j^n \end{cases} \tag{25}$$

The first equation is clearly consistent with a local truncation error $O(\Delta t + \Delta x)$. The second equation corresponds to the up-wind scheme for the transport term since the wind

is assumed to blow from the left to the right, then it is again consistent of order 1.
On the down-wind side $S_j^n \equiv \delta w_j^n$, so we can repeat the same argument and obtain a consistency of order 1.

ii) Stability
On the upwind side we have for w the linear transport equation, subject to the usual CFL condition $\Delta t \leq \frac{\Delta x}{\eta}$. On the downwind side, on the other hand, we have

$$w_j^{n+1} = (1 - \eta\frac{\Delta t}{\Delta x} - \delta\Delta t)w_j^n + \eta\frac{\Delta t}{\Delta x}w_{j-1}^n.$$

In order to have stability in L^∞, we must ask that

$$||w^{n+1}||_\infty \leq \Big(|1 - \eta\frac{\Delta t}{\Delta x} - \delta\Delta t| + \eta\frac{\Delta t}{\Delta x}\Big)||w^n||_\infty \leq ||w^n||_\infty. \tag{26}$$

If $1 - \eta\frac{\Delta t}{\Delta x} - \delta\Delta t \geq 0$ then (26) is satisfied for all $\Delta t > 0$. Otherwise, we must impose

$$-1 + 2\eta\frac{\Delta t}{\Delta x} + \delta\Delta t \leq 1 \quad \text{that implies} \quad \Delta t \leq \frac{2\Delta x}{2\eta + \delta\Delta x}.$$

□

In particular, note that choosing $\Delta t = \frac{\Delta x}{2\eta}$ the scheme is stable for $\Delta x \leq \frac{2\eta}{\delta}$.

Theorem 4.3. *The scheme(*(21) *for Model B* (14) *has the following properties:*
i) is consistent of order 1 in Δt *and* Δx*;*
ii) is stable for

$$\Delta t \leq \frac{2\Delta x}{2\eta + \delta\Delta x + 2\alpha\beta}. \tag{27}$$

Proof. i) Consistency
Let us consider the first equation of model B, note that the the only difference with respect to Model A is given by the second term. In the scheme that term is again discretized by an up-wind finite difference approximation and gives a truncation error of order 1.
The second equation of (14) requires more attention since it contains the second order term

$$(w(\beta h_x - \eta(x)))_x = w_x(\beta h_x - \eta(x)) + w(\beta h_{xx} - \eta_x(x)) \tag{28}$$

(remember that we have introduced a space dependent velocity to take into account the wind attenuation on the down-wind side). Let us focus our attention on the discretization of that term since all the others have been already examined in our analysis. Recalling the definition of ϕ_j^n we can write

$$\begin{aligned} &-\frac{1}{\Delta x}(w_j^n\phi_j^n - w_{j-1}^n\phi_{j-1}^n) \\ &= -\frac{1}{\Delta x}\left[w_j^n\left(\eta_j^n - \beta\left(\frac{h_j^n - h_{j-1}^n}{\Delta x}\right)\right) + w_{j-1}^n\left(\eta_{j-1}^n - \beta\left(\frac{h_{j-1}^n - h_{j-2}^n}{\Delta x}\right)\right)\right] \end{aligned} \tag{29}$$

Now we add and subtract the term $w_{j-1}^n\left(\eta_j^n - \beta\left(\frac{h_j^n - h_{j-1}^n}{\Delta x}\right)\right)$, then after a reorganization of the terms we obtain

$$-\frac{1}{\Delta x}(w_j^n\phi_j^n - w_{j-1}^n\phi_{j-1}^n) = \frac{1}{\Delta x}\left(\frac{w_j^n - w_{j-1}^n}{\Delta x}\right)\left(\beta\frac{h_j^n - h_{j-1}^n}{\Delta x} - \eta_j^n\right) + \tag{30}$$
$$+w_{j-1}^n\left(\left(\beta\frac{h_j^n - 2h_{j-1}^n + h_{j-2}^n}{(\Delta x)^2}\right) - \frac{\eta_j^n - \eta_{j-1}^n}{\Delta x}\right)$$

where one can clearly see the discretization of order 1 for the first derivative of w, h and η and of the second derivative of h appearing in (28). In conclusion, also in this case we obtain consistency of order $O(\Delta t + \Delta x)$.

ii) Stability

Again we can restrict the discussion to the the stability with respect to w, and in particular to what happens on the downwind side, since it gives the strongest restrictions to the choice of Δt. Reasoning as in the proof of the previous theorem, we arrive at the following inequality

$$\left|1 - \eta\frac{\Delta t}{\Delta x} + \beta\frac{\Delta t}{\Delta x}\frac{h_j^n - h_{j-1}^n}{\Delta x} - \delta\Delta t - \gamma\Big(\alpha + \frac{h_j^n - h_{j-1}^n}{\Delta x}\Big)\Delta t\right| + \frac{\Delta t}{\Delta x}\Big(\eta - \beta\frac{h_{j-1}^n - h_{j-2}^n}{\Delta x}\Big) \leq 1$$

where we have used the fact that h is decreasing on the downwind side. If the quantity inside the absolute value is positive, previous inequality is equivalent to the following:

$$\beta\frac{h_j^n - 2h_{j-1}^n + h_{j-2}^n}{\Delta x^2} - \delta - \gamma\Big(\alpha + \frac{h_j^n - h_{j-1}^n}{\Delta x}\Big) \leq 0,$$

relation which is naturally satisfied since the first term (which approximates βh_{xx}) is close to zero on the downwind side where h is essentially linear. If the quantity inside the absolute value is instead negative, then we get

$$\Delta t\Big(\frac{2\eta}{\Delta x} - \frac{2\beta}{\Delta x}\frac{h_j^n - h_{j-2}^n}{2\Delta x} + \delta + \gamma\Big(\alpha + \frac{h_j^n - h_{j-1}^n}{\Delta x}\Big)\Big) \leq 2,$$

that is

$$\Delta t \leq \frac{2\Delta x}{2\eta + \delta\Delta x - 2\beta\frac{h_j^n - h_{j-2}^n}{2\Delta x} + \gamma\Delta x\Big(\alpha + \frac{h_j^n - h_{j-1}^n}{\Delta x}\Big)},$$

where we see the contribution to stability of the new terms in Model B. It is easily seen that the worst situation is when the slope is maximal ($\frac{h_j^n - h_{j-2}^n}{2\Delta x} \simeq -\alpha$), and consequently the last term in the denominator is essentially zero, which gives condition (27). □

As we will see in the next section, condition (27) seems to be too restrictive and it can be relaxed as we will see in the next section.

5 2D numerical tests

5.1 Test Profiles

In order to test the methods, we selected three different initial profiles, whose expressions $h_0(x)$ are listed below and illustrated in Figure 3. Unless for Dune 1, $w_0(x) = w(x, 0) = 0$.

Dune 1: similarity dune (on $\mathbb{R}$ coincides with the traveling dune for Model A)

$$h_0(x) = \begin{cases} \exp(\lambda x) & \text{if } x < 0 \\ \exp(-\mu x) & \text{if } x > 0 \end{cases}, \quad w_0(x) = \epsilon h_0(x)$$

where $\lambda = \frac{\sigma(1+\epsilon)}{\epsilon\eta}$ and $\mu = \frac{\delta}{\eta}(1+\epsilon)$.

Dune 2: 'cosine' dune

$$h_0(x) = \begin{cases} H_0 \cos^2 \frac{\pi}{L_0}(x - C_0) & \text{if } C_0 - \frac{L_0}{2} \le x \le C_0 + \frac{L_0}{2} \\ 0 & \text{otherwise} \end{cases}$$

centered at $x = C_0$, with length L_0 and heigth H_0.

Dune 3: 'arctangent' dune

$$h_0(x) = \begin{cases} \arctan(0.1x) + 1.249 & \text{if } x < 30 \\ -0.2398(x - 40) & \text{if } 30 \le x \le 40 \\ 0 & \text{otherwise} \end{cases}$$

a first convex then concave upwind side, followed by a steep linear downwind side.

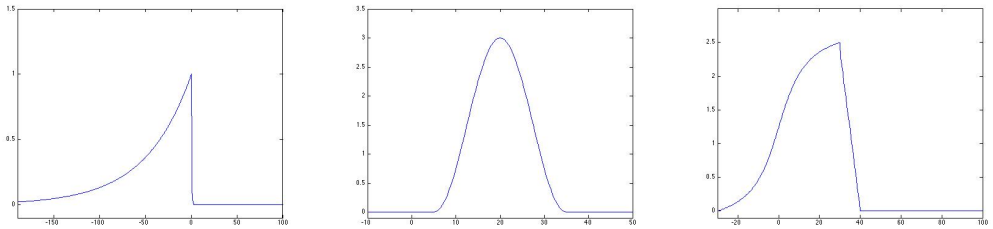

(a) Dune 1 (b) Dune 2 (c) Dune 3

Figure 3: Test profiles

5.2 Numerical Tests for Models A and B

In order to evaluate scheme (19) we show the results obtained for each of the initial profiles of the previous section, using the following set of parameters: $\Delta x = 0.5$, $\eta = 0.5$, $\Delta t = \frac{\Delta x}{2\eta} = 0.5$, $\sigma = 10^{-4}$, $\delta = 1$, $T = 50.000$. In Figure 4 (first row), the evolving dune is plotted every 10.000 time steps, showing the convergence, in finite time, to a stable profile. In its own support, such profile has essentially the shape of the particular similarity solution in $\mathbb{R}$ having same height $h_0 = h_{j_c}^{N_t} := max_j\ h_j^{N_t}$ (the crest height at time T) and layer ratio $\epsilon = w_{j_c}^{N_t}/h_{j_c}^{N_t}$, see (8).This comparison shows that the evolving profiles generated by scheme (19) tend toward a similarity solution of (6), for every initial condition. In other words we can affirm that a similarity solution of suitable height is an *attractive* equilibrium for this model.

We now analyze scheme (21). Since we do not know explicit formulas for the exact solutions of system (14), and we could not prove the existence of a similarity solution in this case, our analysis will remain at a purely qualitative level. That is why we payed attention to the evolution of some parameters which could indicate the formation of a traveling dune also in this case. In particular, for any time t^n we look at:

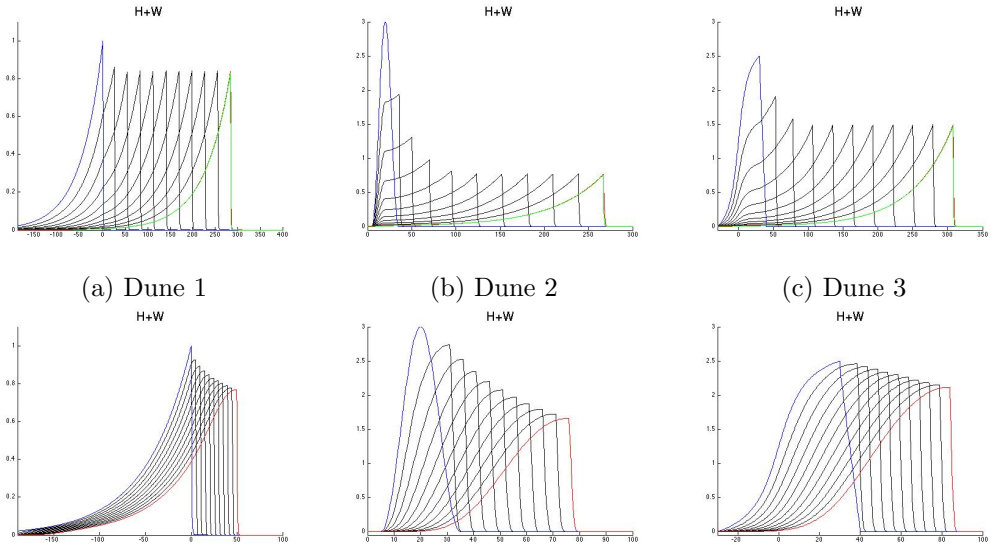

(a) Dune 1 (b) Dune 2 (c) Dune 3

(d) Dune 1 (e) Dune 2 (f) Dune 3

Figure 4: Evolution of test profiles according to Model A (a-c) and Model B (d-f)

- $H^n = h^n_{j_c} = \max_j h^n_j$, the heigth of the dune at the crest node x_{j_c};
- L^n, the length of the dune support, the set where $h^n_j > 0$;
- $\Delta C^n = x_{j_c} - x_{j_0}$, the total crest deplacement, which indicates how far the dune has migrated, and consequently its speed $c^n = \Delta C^n / t^n$;
- ϵ^n, the relative height of the rolling layer with respect to the standing layer, computed at the crest.

In Figure 4, second row, are shown the results of the simulations of the new scheme for the same initial data of Section 5.1 and the same set of parameters mentioned at the beginning of this section (plus $\beta = 0.5$ and $\gamma = 0.1$). Due to the presence of the gravity term, the speed of the dunes is now much lower, so we assumed a larger final time $T = 150.000$, and the evolving dune is plotted every 30.000 time steps.

All tests show the same kind of final profile, in red, which appears (qualitatively) realistic. As expected, the upwind side now consists of an initial convex portion followed by a shorter concave portion. However, for σ large the profile of the upwind side of the dune remains essentially convex, as it was for 'Model A'. The downwind side is entirely convex and much steeper than the upwind side. The dune becomes wider and lower as time progresses, although the loss of height is very small compared to the horizontal displacement between observations.To be more precise, H^n decreases while L^n increases (which is natural, due to the mass conservation), but the derivatives of both these quantities tend to zero, and the crest speed c^n rapidly stabilizes (in Table 1 values of these indicators are listed every 130.000 time steps in a test for Dune 2 on a very long time $T = 1.300.000$, see also Figure 5).

This fact, along with the similar profile that all the dunes in the tests assume as time progresses (even for quite different initial data), let indeed conjecture the asymptotic

$k(t^n = 130.000k)$	H^n	L^n	ΔC^n	$c^n(\times 10^{-4})$	$\epsilon^n(\times 10^{-3})$
1	0.72	97	96	3.69	1.42
2	0.51	147	190	3.65	1.44
3	0.41	184	284	3.64	1.40
4	0.36	216	378	3.64	1.46
5	0.32	243	474	3.64	1.09
6	0.29	267	568	3.64	1.46
7	0.27	289	664	3.65	1.23
8	0.25	310	759	3.65	1.31
9	0.236	329	854	3.65	1.47
10	0.224	347	949	3.65	1.40

Table 1: Shape parameters of Dune 2 for long time evolution

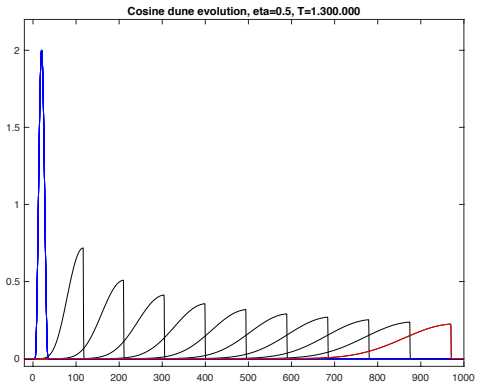

Figure 5: Long time evolution of Dune 2 with Model B

convergence of the evolving profiles toward a sort of similarity dune even for this model. A rigorous proof of that property is still an open problem.

Remark 1. Experiments show that condition (27) for stability of scheme (21) is a little bit too restrictive, since in practice for many choices of the parameters the maximal slope of the dune in the downwind side remains strictly below α. When β is small compared to η, in general (24) is still sufficient for stability even in this case, but when the gravity effect becomes more relevant a stronger condition is needed (see Table 2). The wind speed is not strong enough to move the eroded sand in the right direction, and the used upwind approach becomes unstable. We finally remark that the parameter γ is not so relevant for stability, since it is in general very small compared to the others.

The last column Δt_{max} shows the smaller time step Δt for which blow up occurs, so to have stability one has to choose a Δt lower than that threshold. Note that condition (24) is not enough for stability, even if (27) remains too restrictive.
In the experiments we have have also tested the effects of varying some key parameters in model B. Here are some comments.

Δx	β	η	(24)	(27)	Δt_{max}
0.5	0.5	0.25	1	0.59	0.83
	0.5	0.5	0.66	0.45	0.71
	1	0.5	0.66	0.35	0.56
	2	0.5	0.66	0.23	0.44
0.25	0.5	0.25	0.66	0.35	0.44
	0.5	0.5	0.4	0.26	0.4
	1	0.5	0.4	0.19	0.28
	2	0.5	0.4	0.12	0.22
0.125	0.5	0.5	0.22	0.13	0.19
	1	0.5	0.22	0.10	0.15

Table 2: Stability test for Dune 2 for different choices of the parameters with $\beta \geq \eta$

Effect of η. To see the effect of the transport speed η, we fixed all the other parameters except Δt, which is chosen in order to keep constant the CFL condition. For a fixed time T the basic shape of the final dune remains the same, but if the transport speed increases the dune moves more rapidly and flattens out in time, becoming wider and smaller. The distance of the dune displacement appears to be a linear function of the transport speed. The total distance traveled, on the other hand, depends on the shape of the initial dune. Also the speed of the dune varies linearly with η, but it does *not* depend on the initial condition.

Effect of γ. Increasing the exchange rate γ has the opposite effect on the dunes with respect to η. This is to be expected, a lower exchange rate makes more grains remain in the rolling layer rather than being lost to the standing layer. As a consequence this makes the dune move faster. In conclusion, the dune motion can be increased in two ways: by increasing the speed and/or by decreasing the exchange rate.

5.3 Multiple dunes

Dunes are not usually found isolated in nature, but rather in areas known as *dune fields* in which many dunes move together. That is why in this subsection we present some tests made in order to adapt Model B to that general case. Multiple dunes means many crests with different heights, and one has to consider the interactions among them. In other words, one has to determine which part of the rising surface of a dune is not subjected to erosion because it is protected from the wind by another dune. Assume to have a sequence of m dunes with crests position $\widehat{x}_i$ and height $\widehat{h}_i = h(\widehat{x}_i)$, for $i = 1, .., m$. We adopted the following strategy: the rising surface of the $(k+1)-$th dune is considered an *upwind region* only for the part which emerges from the wind protection area induced by the k-th dune, that is if $h_x(x) > 0$ and $h(x) > s_k(x)$, where $s_k(x)$ denotes the profile of the protection area related to the k-th dune. We tested two different shapes for that (see Figure 6), which gave similar results in the tests:

$$s_k(z) = \widehat{h}_k(1 - z) \qquad (\textit{linear case}),$$

$$s_k(z) = 2\widehat{h}_k z^3 - 3\widehat{h}_k z^2 + \widehat{h}_k \qquad (\textit{separation bubble}),$$

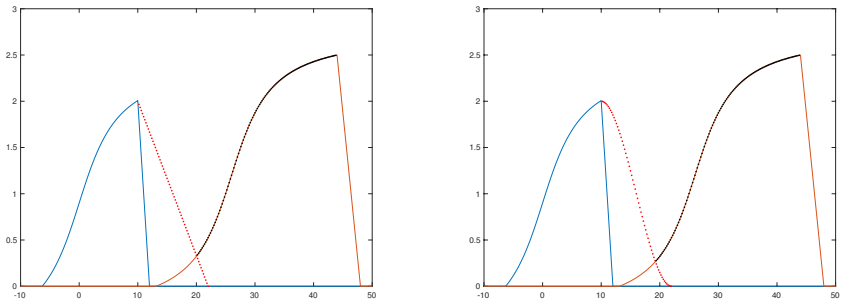

Figure 6: Wind protection effects between two successive dunes. For the second dune erosion is active only on the black region: a) linear case, b) separation bubble.

where $z = \frac{x-\widehat{x}_k}{L_k} \in [0,1]$, and L_k denotes the width of the protection area, for example $L_k = 6\widehat{h}_k$ (it is known from the literature, see for example [15], that wind protection area after a crest of height $\widehat{h}$ has approximately a length of six times $\widehat{h}$). The cubic polinomial in the second choice of s_k is a simplified version of the separating streamline used in [15] and shown in Fig.1.

The definition (12) of the transport speed $\eta(x)$ has been modified in a similar way: equal to $\bar{\eta}$ in each upwind region, and linearly decreasing in between two subsequent dunes.

We present the evolution of three sets of initial dunes, with same or different heights:

$$1)\ h_0(x) = \max(\sin\frac{x}{10}, 0) \ \text{ if } x < 160, \quad h_0(x) = 0 \quad \text{elsewhere;}$$

$$2)\ h_0(x) = \max(\sin\frac{x}{10} + 2\cos\frac{x}{13}, 0) \ \text{ if } x < 200, \quad h_0(x) = 0 \quad \text{elsewhere;}$$

$$3)\ h_0(x) = \max(\frac{x(20-x)}{20}, \frac{(x-18)(45-x)}{45}, \frac{(x-35)(64-x)}{55}, 0) \ \text{ if } x \in [0,100].$$

The corresponding results are shown in Fig.7-9.

In the first two cases three distinct initial dunes travel separately and progressively merge together; in the third case the starting profile is a single dune with three crests of different heights. The simulation shows that after some time the second one incorporates the third and later on the first one overcomes and includes their union remaining a single traveling dune. In the first frame it is possible to see the effects of the wind protection area between the first two crests.

6 A Three-Dimensional Extension

The main interest is of course to have a complete 3D model for dune migration, in order to simulate the formation and the traveling of one or more barchan dunes. The extension of Model B to this case, the discussion of its properties, together with the results of many numerical simulations, will be the object of a forthcoming paper [8]. Here we just anticipate some of its basic features. Of course, h and w now become functions of x, y, and t, and some changes are very natural: since the slope of the dune cannot exceed the angle of repose, we have that grains leave the standing layer and enter the rolling layer if

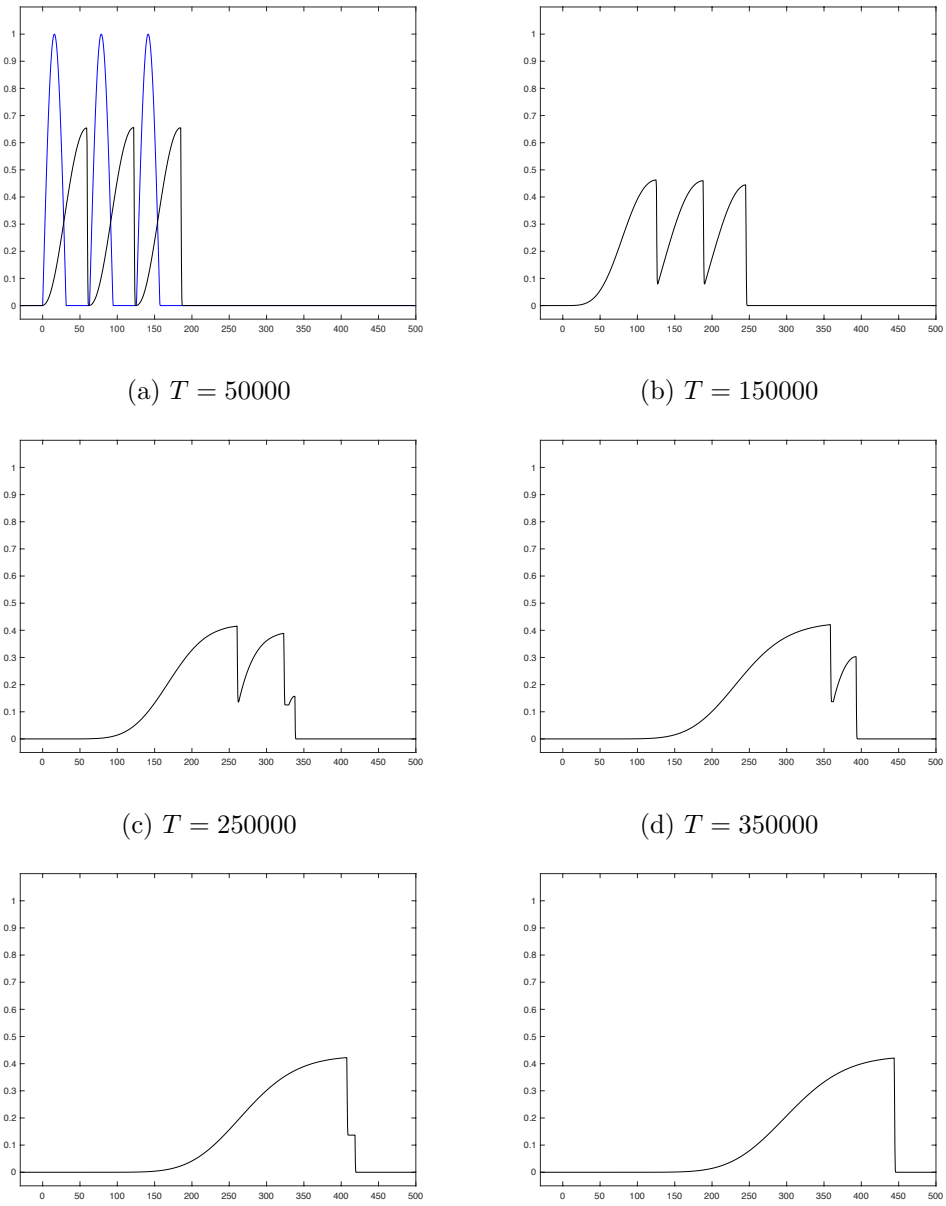

(a) $T = 50000$ (b) $T = 150000$

(c) $T = 250000$ (d) $T = 350000$

(e) $T = 400000$ (f) $T = 450000$

Figure 7: Evolution of three initial dunes with same height

$|\nabla h| > \alpha$. Similarly, the direction of descent of rolling grains which move downhill due to gravity is the direction of steepest descent in every point, i.e. $-\nabla h$.

We assume as before that the wind has no vertical component, but now the transport velocity is a vector $\vec{\eta} = (\eta_1, \eta_2)$, where η_1 and η_2 denote the transport speeds along the x and the y axis respectively (unlike the Model B, we decided to take them constant).

The very delicate task is how to determine which areas of the dune should be considered upwind or downwind, that is which ones are exposed to the wind. For that we make use of the normal vector. If we describe the surface of the standing layer through the equation

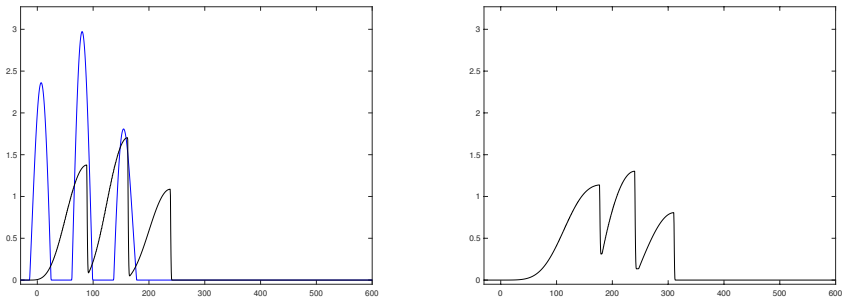

(a) $T = 100000$

(b) $T = 200000$

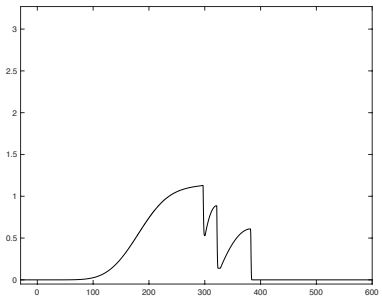

(c) $T = 300000$

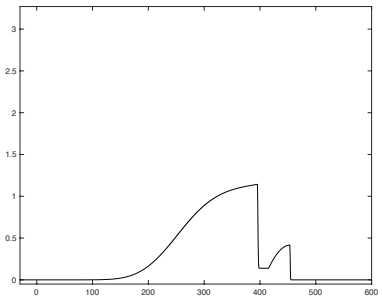

(d) $T = 400000$

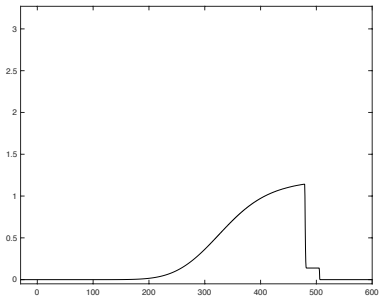

(e) $T = 500000$

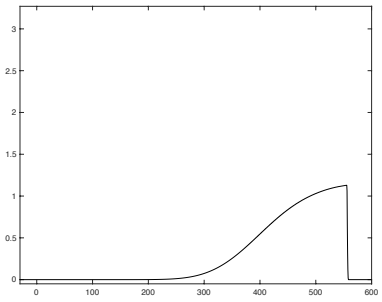

(f) $T = 600000$

Figure 8: Evolution of three initial dunes with different height

$F(x, y, z) = z - h(x, y, t) = 0$, the unit exterior normal vector is given by

$$\vec{N} = \frac{(F_x, F_y, F_z)}{\sqrt{F_x^2 + F_y^2 + F_z^2}} = \frac{(-h_x, -h_y, 1)}{\sqrt{h_x^2 + h_y^2 + 1}}.$$

Projecting this vector onto the (x, y) plane, we obtain

$$\vec{n} = \frac{(-h_x, -h_y)}{\sqrt{h_x^2 + h_y^2}},$$

through which we are now able to distinguish the sides of the dune. The crest will be no longer a single point but a curve in the three-dimensional space. A generic point $(\bar{x}, \bar{y})$

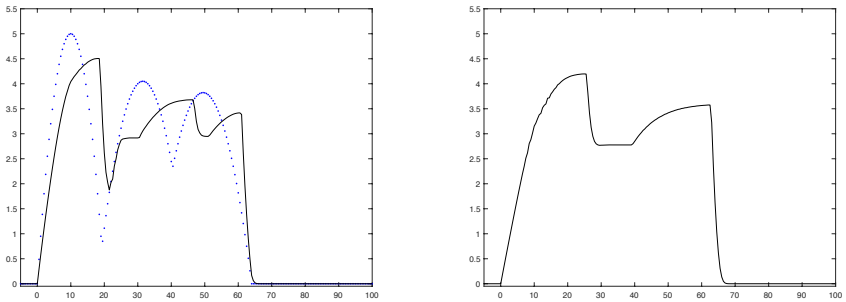

(a) $T = 5000$

(b) $T = 10000$

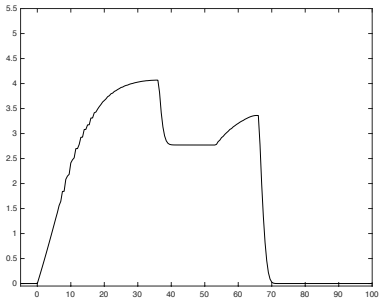

(c) $T = 15000$

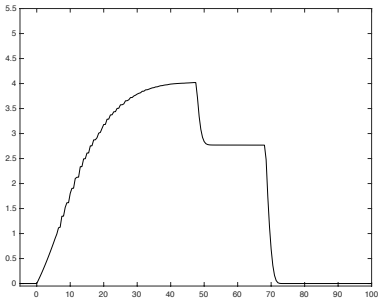

(d) $T = 20000$

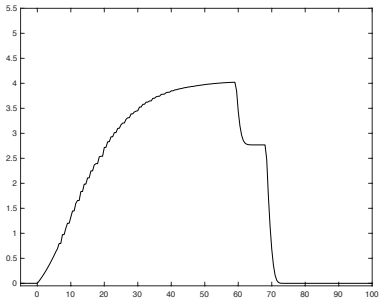

(e) $T = 25000$

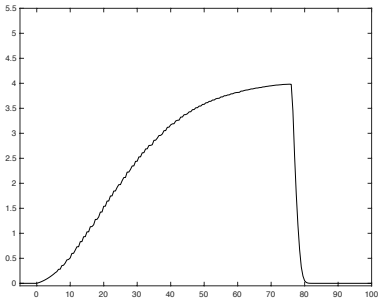

(f) $T = 40000$

Figure 9: Evolution of a single initial dune with three crests of different height (graph in dots)

will be considered in the upwind region (luff) if the angle ϕ between the transport velocity $\vec{\eta}$ and the projected normal vector $\vec{n}$ is between $\frac{\pi}{2}$ and π. In fact, since the transport velocity is null along the z axis, it suffices to look at a section of the dune parallel to the (x, y) plane. If $\frac{\pi}{2} \leq \phi \leq \pi$ the wind can blow over the dune at that point and to erode the dune. On the contrary, if $0 < \phi < \frac{\pi}{2}$ at the point, then the wind is blocked by the dune so that point belongs to the downwind region (lee). For example, A in Fig. 10 is an upwind point, while B is a downwind point.

Since the dot product between two vectors v and w in $\mathbb{R}^2$ is given by $v \cdot w = |v||w| \cos \phi$, where ϕ is the angle between them, the angle between the transport speed and the normal

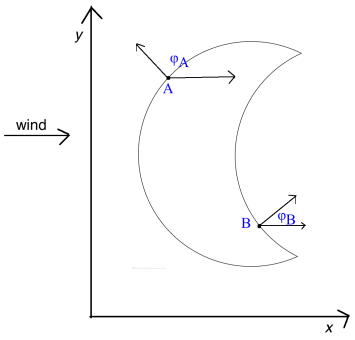

Figure 10

vector is given by

$$\phi = \arccos\left\{\frac{\vec{\eta}}{|\vec{\eta}|}\cdot\vec{n}\right\} = \arccos\left\{\frac{-\eta_1 h_x - \eta_2 h_y}{\sqrt{\eta_1^2+\eta_2^2}\sqrt{h_x^2+h_y^2}}\right\}. \tag{31}$$

Remark 2. If the wind is unidirectional and coincides with the x axis, then $\vec{\eta} = (\eta_1, 0)$, and the upwind part of the dune is again where $h_x > 0$, as it was for Model B.

In conclusion, the three-dimensional model becomes:

Model C

$$\begin{cases} \frac{\pi}{2} \le \phi \le \pi & \begin{cases} h_t = -\sigma h + \gamma(\alpha - |\nabla h|)w \\ w_t = \nabla(w(\beta\nabla h - \vec{\eta})) + \sigma h - \gamma(\alpha - |\nabla h|)w \end{cases} \\ 0 < \phi < \frac{\pi}{2} & \begin{cases} h_t = (\gamma(\alpha - |\nabla h|) + \delta)w \\ w_t = \nabla(w(\beta\nabla h - \vec{\eta})) - (\gamma(\alpha - |\nabla h|) + \delta)w \end{cases} \end{cases} . \tag{32}$$

where ϕ is given by (31).

As a test we show the evolution of an initial dune $h_0(x, y)$ with the shape of an hyperboloid of two sheets centered in $(0, 0)$ and with compact support in $\Omega = [-15, 55] \times [-30, 30]$ (see Fig. 11.a).

$$h_0(x, y) = \max\left\{0, 4 - \sqrt{4 + \frac{x^2+y^2}{9}}\right\}.$$

We assume that the wind is blowing from the West and observe the migration and deformation of the dune at a final time of $T = 50.000$ (here are all the parameters: $\eta_1 = 0.25$, $\eta_2 = 0$, $\beta = 0.5$, $\sigma = 10^{-4}$, $\delta = 1$, $g = 0.1$, $\Delta x = 0.5$, $\Delta t = 0.5$). The final level sets for h and w are shown in Fig. 11, together with some horizontal slices of the the dunes, in particular along $y = 0$, $y = 5$, $y = 10$, and $y = 15$ at time T. In these case the dunes is of course symmetrical with respect to the x axis.

7 Conclusions

We have described the migration of sand dunes in the simplified 2D settings, both on a physical and on a numerical level. Our Model B extends the simple model presented in

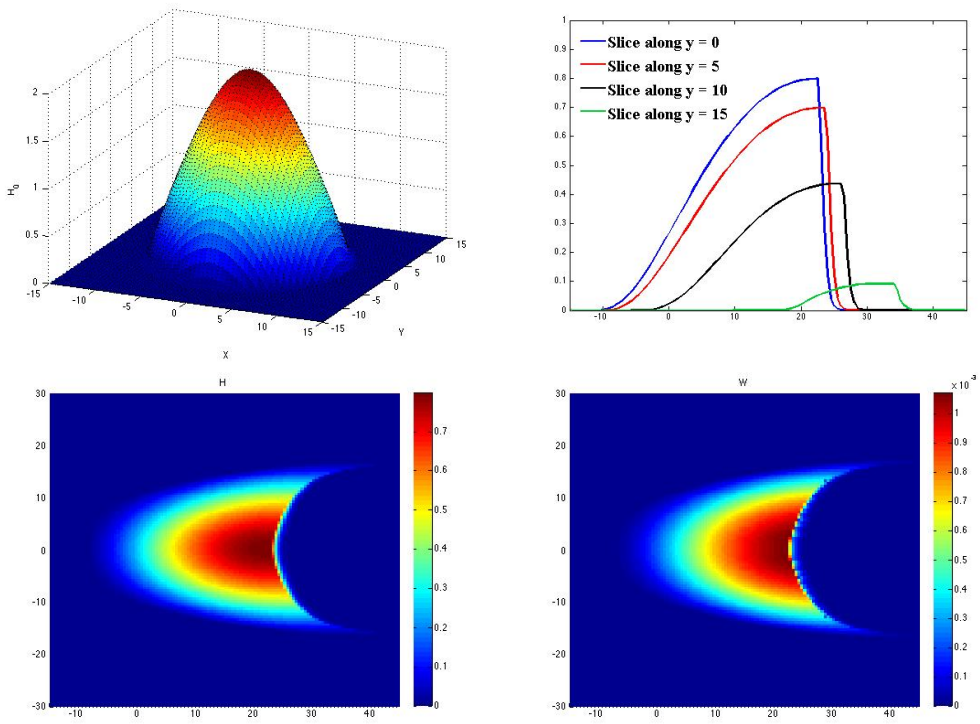

Figure 11: A 3D test: a) initial profile (hyperboloid); b-c-d) horizontal slices, h and w layers (from above) at time T=50000

[12] showing in the numerical experiments a more realistic evolution for the dune and a stable asymptotic behavior. In order to better describe real-life dunes, it will of course be necessary to set all the parameters according to experimental data but we do not have this information. Hopefully in the future we could have access to real physical data.

Even if the model still describes a very simplified version of the phenomenon, it is interesting to say that, due to the closed form of the model, the numerical simulation is much quicker, and the execution time for different initial data much more uniform than the one used for example by the application of the Minimal Model M that requires several steps to complete the simulation.

More work certainly needs to be done, especially on extensions of such a model to the three-dimensional case, also to consider multiple wind sources or time-dependent winds, since the current model does not account for that.

We plan to develop a more detailed analysis of this extension and of its discretization in a forthcoming paper [8].

References

[1] Andreotti B., Claudin P. and Douady S., *Selection of dune shapes and velocities. Part 1: Dynamics of sand, wind and barchans*, Eur. Phys. J. B 28 (2002), 321-339.

[2] Araújo A.D., Parteli E.J.R., Poschel T., Andrade Jr. J.S. and Herrmann H.J., *Numerical modeling of the wind flow over a transverse dune*, Sc. Report 3, art. 2858 (2013)

[3] Bagnold R.A., The physics of blown sand and desert dunes, Methuen, London, 1954

[4] Bouchaud J.P., Cates M.E., Ravi Prakash J. and Edwards S.F., *A Model for the Dynamics of Sandpile Surfaces*, J. Phys. I France, 4 (1994), 1383-1410.

[5] Caboussat A. and Glowinski R., *A Numerical Method for a Non-Smooth Advection-Diffusion Problem Arising in Sand Mechanics*, Commun. Pure Appl. Anal., 8 (2009), 161-178.

[6] Falcone M. and Finzi Vita S., *A finite difference approximation of a two-layers system for growing sandpiles*, SIAM J. Scientific Computing, Vol. 28, No. 3 (2006), 1120-1132.

[7] Falcone M. and Finzi Vita S., *A semi-Lagrangian scheme for the open table problem in granular matter theory*, in K. Kunisch, G. Of, O. Steinbach (eds.), Numerical Mathematics and Advanced Applications, (Proceedings of ENUMATH 2007, Graz, Austria, September 10-14, 2007), Springer, Berlin Heidelberg, 2008, 711-718.

[8] Falcone M. and Finzi Vita S., *Modeling sand dunes evolution via a two layer model*, in progress

[9] Guignier L., Niiya H., Nishimori H, Lague D. and Valance A., *Sand dunes as migrating strings*, Physical Review E 87, 052206 (2013)

[10] Haack F., *Modeling Sand Dune Dynamics: a Theoretical and Numerical Study*, Master Thesis in Mathematics for Applications, Sapienza University of Rome, 2015.

[11] Hadeler K.P. and Kuttler C., *Dynamical models for granular matter*, Granular Matter, **2** (1999), 9-18.

[12] Hadeler K.P. and Kuttler C., *Granular matter*, int. report U. Tübingen n. 185 (2003)

[13] Hersen P., *On the crescentic shape of barchan dunes*, Eur. Phys. J. B 37 (2004), 507-514.

[14] Jackson P.S. and Hunt J.C.R., *Turbulent wind flow over a low hill*, Quart J.R. Met. Soc., 101 (1975), 929-955.

[15] Kroy K., Sauermann G. and Hermann H.J., *Minimal model for aeolian sand dunes*, Physical Review E 66, 031302 (2002)

[16] Lo Giudice A., Giammanco G., Fransos D. and Preziosi L., *Modelling Sand Slides by a Mechanics-Based Degenerate Parabolic Equation*, Mathematics and Mechanics of Solids, (2018), 1081286518755230.

[17] Ortiz P. and Smolarkiewicz P.K., *Coupling the dynamics of boundary layers and evolutionary dunes*, Physical Review E 79, 041307 (2009)

[18] Prigozhin L., *Variational model of sandpile growth*, Euro. J. Applied Mathematics 7 (1996), 225-235.

[19] Sauermann G., Kroy K. and Hermann H.J., *A continuum saltation model for sand dunes*, Physical Review E 64, 031305 (2001)